

# Final Version of the Physics-Dynamics Coupling

I. Martínez Marco, INM

9th November 2004

## Introduction

- This note describes a partial second-order accurate approximation of the physical parametrizations in the two-time-level semi-Lagrangian and semi-implicit (2TLSLSI) version of the HIRLAM model.
- The approximation is achieved by averaging the total parameterization tendencies along the semi-Lagrangian trajectory, following the ECMWF approach (Wedi,1999).
- The coupling of the physics to the dynamics in the HIRLAM model is described and compared with the current operational configuration.
- A "first-guess" predictor of the model variables is employed to achieve the coupling of the different parametrization schemes with each other.

## Coupling of parameterizations with the dynamics

The generic one-dimensional advection equation can be written as:

$$\frac{\partial\psi(x,t)}{\partial t} + u(x,t)\frac{\partial\psi(x,t)}{\partial x} = L\{\psi(x,t)\} + N\{\psi(x,t)\} \quad (1)$$

where  $\psi$  is a scalar field,  $u$  is the advecting velocity and  $L$  and  $N$  represent the linear and nonlinear terms, respectively.

Following McDonald(1998), the 2TLSLSI method of discretization can be expressed as:

$$\psi_I^{n+1} - \psi_*^n = \frac{\Delta t_+}{2}[L^{n+1} + N^{n+\frac{1}{2}}]_I + \frac{\Delta t_-}{2}[L^n + N^{n+\frac{1}{2}}]_* \quad (2)$$

where  $N^{n+\frac{1}{2}} = \frac{(3N^n - N^{(n-1)})}{2}$

and  $\Delta t_{\pm} = (1 \pm \epsilon_g)\Delta t$ ;  $\epsilon_g$  is called the "decentering" parameter (to reduce high-frequency oscillations). For any field  $\phi$ ,  $\phi_I^n = \phi(I\Delta x, n\Delta t)$ , and  $\phi_*^n = \phi(x_*, n\Delta t)$ . The subscripts I and \* denote, respectively, an evaluation at the arrival point and the departure point of the trajectory. The superscript n denotes the number of time-step.

If physical parameterizations are also included and following the ECMWF approach, the resulting equation is:

$$\psi_I^{n+1} - \psi_*^n = \frac{\Delta t_+}{2}[L^{n+1} + N^{n+\frac{1}{2}} + P^{n+1}]_I + \frac{\Delta t_-}{2}[L^n + N^{n+\frac{1}{2}} + P^n]_* \quad (3)$$

- where one half of the tendency is computed at the arrival point and the other half at the departure point of the trajectory. This approximation is second-order accurate.
- The current reference HIRLAM model makes use only of the parameterization tendencies at the arrival point, being thus the time discretization only first-order accurate for physical processes.

## Physics-Dynamics Coupling strategy

- Coupling experiment: the contributions of the radiation, convection and vertical diffusion schemes are averaged along the semi-Lagrangian trajectory in all the equations.

The final equation, once the tendencies of the parameterizations are computed, is:

$$\psi_I^{n+1} - \psi_D^{n+1} = \frac{\Delta t_+}{2}[P_{rad+conv+vdif}^{n+1}]_I + \frac{\Delta t_-}{2}[P_{rad+conv+vdif}^n]_* \quad (4)$$

where  $\psi_D^{n+1}$  stands for the dynamical fields at the arrival point.

- In the current reference HIRLAM model (**REF** experiment), the contributions of the radiation, convection and vertical diffusion schemes are taken at the arrival point only.

The final equation is:

$$\psi_I^{n+1} - \psi_D^{n+1} = \Delta t[P_{rad+conv+vdif}^{n+1}]_I \quad (5)$$

## Coupling of the parameterization schemes

- The HIRLAM model makes use of the "fractional stepping" approach (Beljaars, 1991). The results depend consequently on the calling sequence.

- In the HIRLAM model this sequence is: first, radiation; second, soil processes; third, vertical diffusion and, lastly, convection. The convection scheme, therefore, uses the tendencies of the vertical diffusion and radiation schemes.
- To maintain the idea of "fractional stepping", a "first guess" predictor of the model variables is used.
- The coupling depends on the parametrization schemes implemented in the model. Several "first guess" predictors will be tested to increase the coupling between these schemes:
  - In the **WAL** experiment, a "first guess" predictor is employed by using the tendency from the dynamics and the tendencies of the radiation, vertical diffusion and convection at the previous time-step (Martínez, 2004):

$$\psi_{predict}^{n+1} = \psi_D^{n+1} + 0.5P_{*,rad+conv+vdiff}^n \Delta t \quad (6)$$

- In the **WAB** experiment, a new "first guess" predictor is employed by using the tendency from the dynamics, the tendencies of the radiation, vertical diffusion and convection at the previous time-step and the tendencies of the radiation and vertical diffusion at the current time-step:

$$\psi_{predict}^{n+1} = \psi_D^{n+1} + 0.5P_{*,rad+conv+vdiff}^n \Delta t + 0.5P_{I,rad+vdiff}^{n+1} \Delta t \quad (7)$$

- In the **WAC** experiment, a new "first guess" predictor is employed by using the tendency from the dynamics, the half of the tendency of the convection at the previous time-step and the tendencies of the radiation and vertical diffusion at the current time-step:

$$\psi_{predict}^{n+1} = \psi_D^{n+1} + 0.5P_{*,conv}^n \Delta t + P_{I,rad+vdiff}^{n+1} \Delta t \quad (8)$$

In the proposed schemes the parameterizations at the current time-step are computed in the following calling sequence:

$$P_I^{n+1} = P_{I,rad}^{n+1}(\psi^n) + P_{I,vdiff}^{n+1}(\psi_D^{n+1}) + P_{I,conv}^{n+1}(\psi_{predict}^{n+1}) \quad (9)$$

The current reference HIRLAM model (**REF** experiment) uses "fractional stepping" with the following calling sequence:

$$\psi_{predict}^{n+1} = \psi_D^{n+1} + P_{I,rad}^{n+1} \Delta t + P_{I,vdiff}^{n+1} \Delta t \quad (10)$$

$$P_I^{n+1} = P_{I,rad}^{n+1}(\psi^n) + P_{I,vdiff}^{n+1}(\psi_D^{n+1}) + P_{I,conv}^{n+1}(\psi_{predict}^{n+1}) \quad (11)$$

- Radiation and vertical diffusion schemes remain unchanged.
- The main difference between the preceding experiments is the value of the first-guess used in the convection scheme.

In order to improve the implicitness of the formulation with respect to the vertical diffusion, a second call to this scheme was implemented. The vertical diffusion is called again after the other physical processes have been computed using them as source terms:

- **WAD** experiment = **WAB** experiment + second call to vertical diffusion
- **WAP** experiment = **WAC** experiment + second call to vertical diffusion

## Comparison of numerical accuracy

- The **WAL**, **WAB**, **WAC**, **WAD** and **WAP** experiments are compared to the **REF** one:
  - HIRLAM version 6.2,
  - 0.2°x0.2° resolution in the horizontal,
  - 40 hybrid levels in the vertical and
  - 326x125 points.
- Mixed (Cubic/Linear) interpolation is used to interpolate the diabatic tendencies P to the departure point of the semi-Lagrangian trajectory.
- In the first time step, the configuration is similar to the reference HIRLAM model.
- To examine the sensitivity of the solutions to changes in the length of the time-step, we assume that the method which has the long time-step solution closer to the short time-step solution is the better method (Wedi,1999).
- Four different 24-hour forecasts have been run with t=60s and t=450s. As a measure for the deviation of the 450s-solution from the assumed correct 60s-solution, the root mean square error has been computed for the six experiments:

$$rmse = \sqrt{\overline{(F_{t=450s} - F_{t=60s})^2}} \quad (12)$$

The overbar denotes an average over area. The variables F are the diabatic tendencies integrated vertically and accumulated every time-step over a period of 24 hours.

Comparing **WAL**, **WAB**, **WAC** and **REF** experiments, we get:

- The rmse of all the coupling experiments is smaller than the one of the reference version. The WAB and WAC experiments show better rmse than the WAL one (figure 1). The rmse of the diabatic tendencies of temperature, specific humidity and cloud water content due to vertical diffusion in the WAB and WAC experiments are smaller than the ones in the WAL and REF experiments (figure 1 on the right). In particular, the rmse of the diabatic tendency of the cloud water content due to vertical diffusion improves with the new "first-guess" of the WAC experiment (figure 1 on the centre right).

Comparing **WAC**, **WAP** and **REF** experiments, we get:

- The rmse of the coupling experiments with and without second call to vertical diffusion are very similar. The rmse of the diabatic tendency of cloud water content due to vertical diffusion is even worse with the second call (figure 2).

## Verification scores

Four parallel runs have been carried out with **WAL**, **WAC**, **WAP** and **REF** experiments.

The general characteristics are:

- HIRLAM version 6.2,
- domain of the RCR model,
- 406x324 points with a 0.2°x0.2° resolution in the horizontal,
- 40 hybrid levels in the vertical,
- time step t=300s and
- from 16.11.2003 1200 UTC to 15.12.2003 1200 UTC up to H+48.

Verification scores against observations over the EWGLAM area have been carried out to compare the different schemes.

The WAL experiment shows slightly worse scores than the REF one at 500 hPA temperature and wind at 48-hour forecast and quite similar scores in the other vertical profiles (Martínez, 2004)(figure 3).

By comparing WAC and REF experiments, the vertical profiles of the verification scores are very similar at all the forecast lengths, improving the results of the WAL experiment. The vertical profile of the dew point temperature at 48-hour forecast is slightly better than with the REF experiment (figure 4).

The WAC and WAP experiments, coupling without and with second call to the vertical diffusion respectively, show similar scores. This second call does not seem to improve the verification scores (figure 5).

## Conclusions

The contributions of the radiation, convection and vertical diffusion schemes averaged along the semi-Lagrangian trajectory in all the equations have been chosen as the physics-dynamics coupling strategy.

The numerical accuracy and the verification scores have been improved by using a new "first-guess" predictor that employs the tendency from the dynamics, the half of the tendency of the convection at the previous time-step and the tendencies of the radiation and vertical diffusion at the current time-step.

The results, with and without second call to the vertical diffusion, have been alike. It seems that this second call has not improved the coupling outputs.

The Physics-Dynamics Coupling leads to:

- more stable results,
- similar accurate results for short time-step and more accurate ones for long time-step,
- a smoothing of the fields, especially precipitation and
- appreciable improvements in the medium range forecast skill, although not so noticeable in the short range.

## References

Beljaars, A., 1991: Numerical Schemes for Parameterizations, Proceedings of the ECMWF Seminar on Numerical Methods in Atmospheric Models, Reading, pp.1-42.

Martínez, I., 2004: Tests prior to the operational implementation of the Physics-Dynamics Coupling. HIRLAM Newsletter No. 45, pp. 184-198.

McDonald, A.,1998: The Origin of Noise in Semi-Lagrangian Integrations. Proceedings of the ECMWF Seminar on Recent Developments in Numerical Methods for Atmospheric Modelling, Reading, pp. 308-334.

Wedi, N.P., 1999: The Numerical Coupling of the Physical Parametrizations to the Dynamical Equations in a Forecast Model, Technical Memorandum No.274, ECMWF.

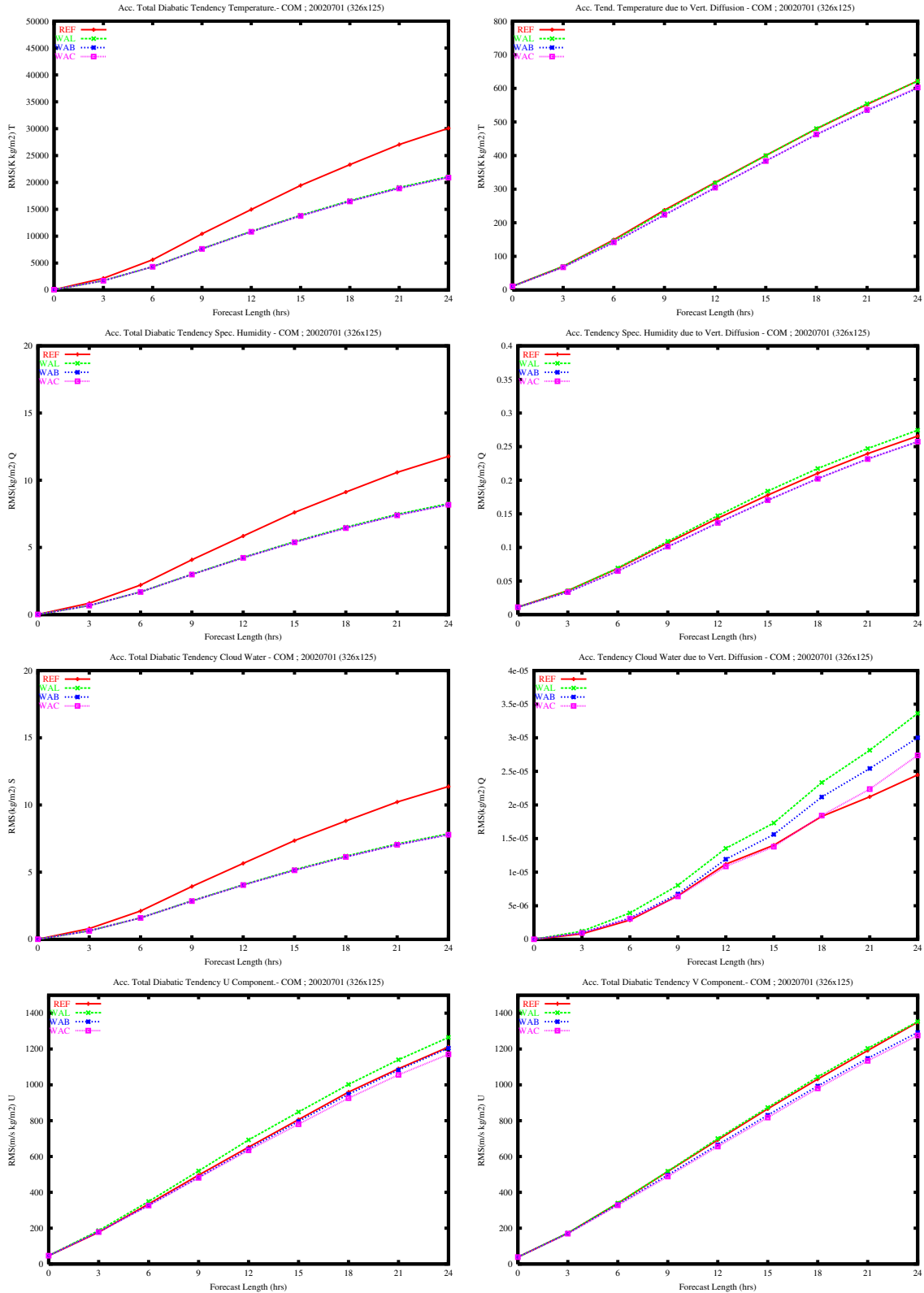


Figure 1: RMSE of the accumulated total diabatic tendency of temperature (*top left*), specific humidity (*centre left*), cloud Water Content (*centre left*), U wind component (*bottom left*) and V wind component (*bottom right*) and RMSE of the diabatic tendencies of temperature (*top right*), specific humidity (*centre right*) and cloud water content (*centre right*) due to vertical diffusion.

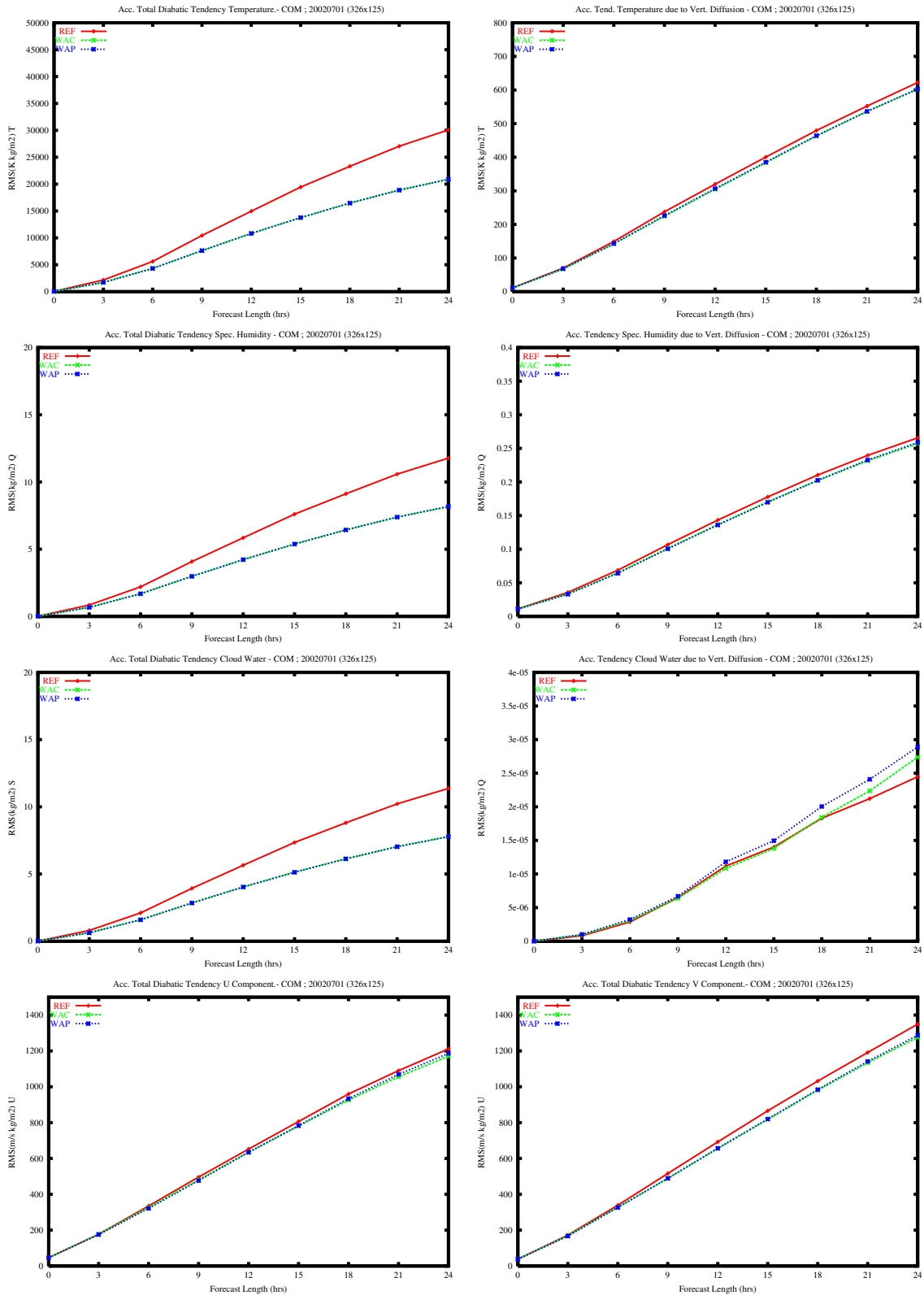


Figure 2: RMSE of the accumulated total diabatic tendency of temperature (*top left*), specific humidity (*centre left*), cloud Water Content (*centre left*), U wind component (*bottom left*) and V wind component (*bottom right*) and RMSE of the diabatic tendencies of temperature (*top right*), specific humidity (*centre right*) and cloud water content (*centre right*) due to vertical diffusion.

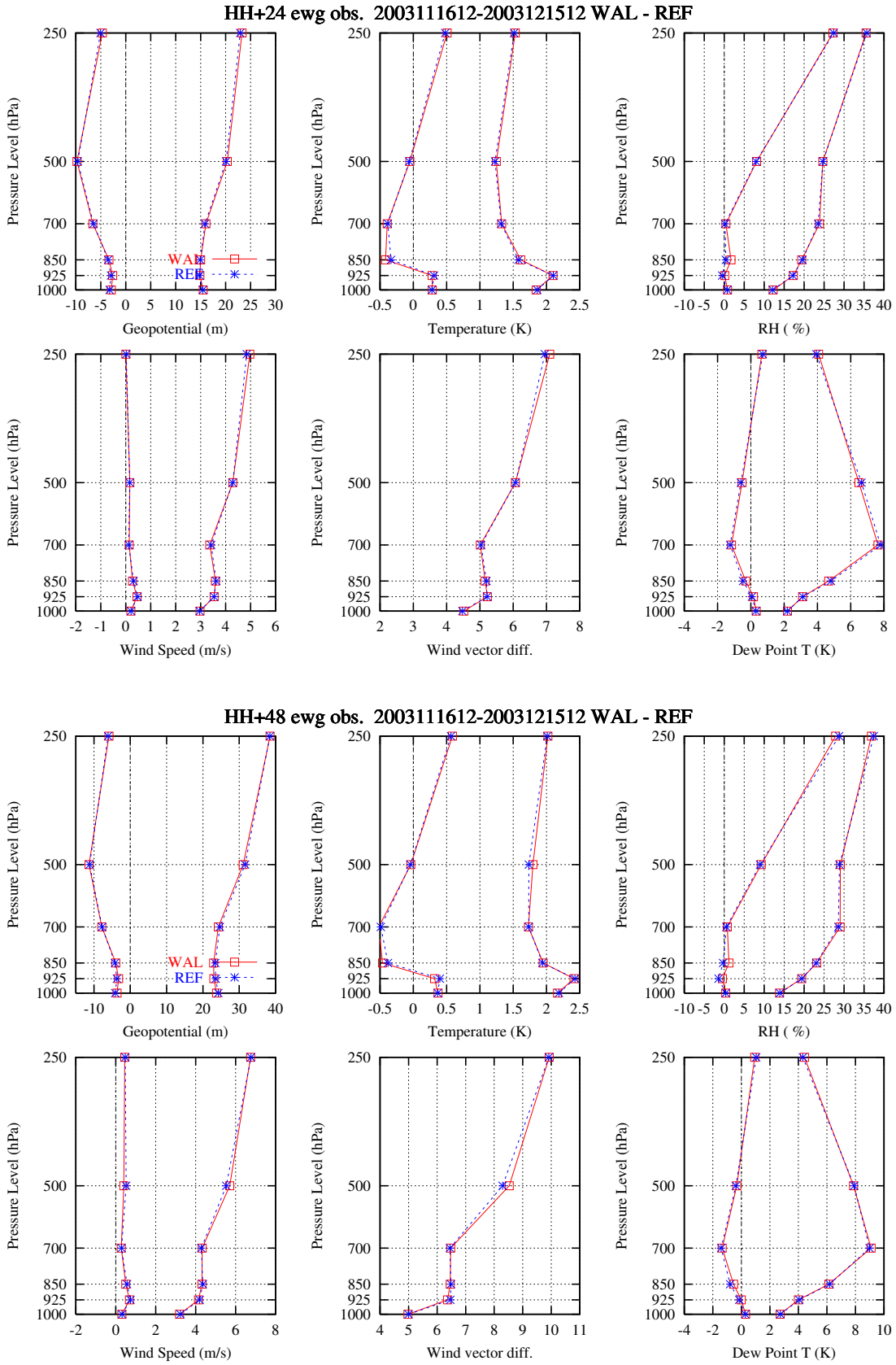


Figure 3: Vertical profiles of the verification scores at 24-hour forecast (*top*) and at 48-hour one (*bottom*) of the WAL and REF experiments.

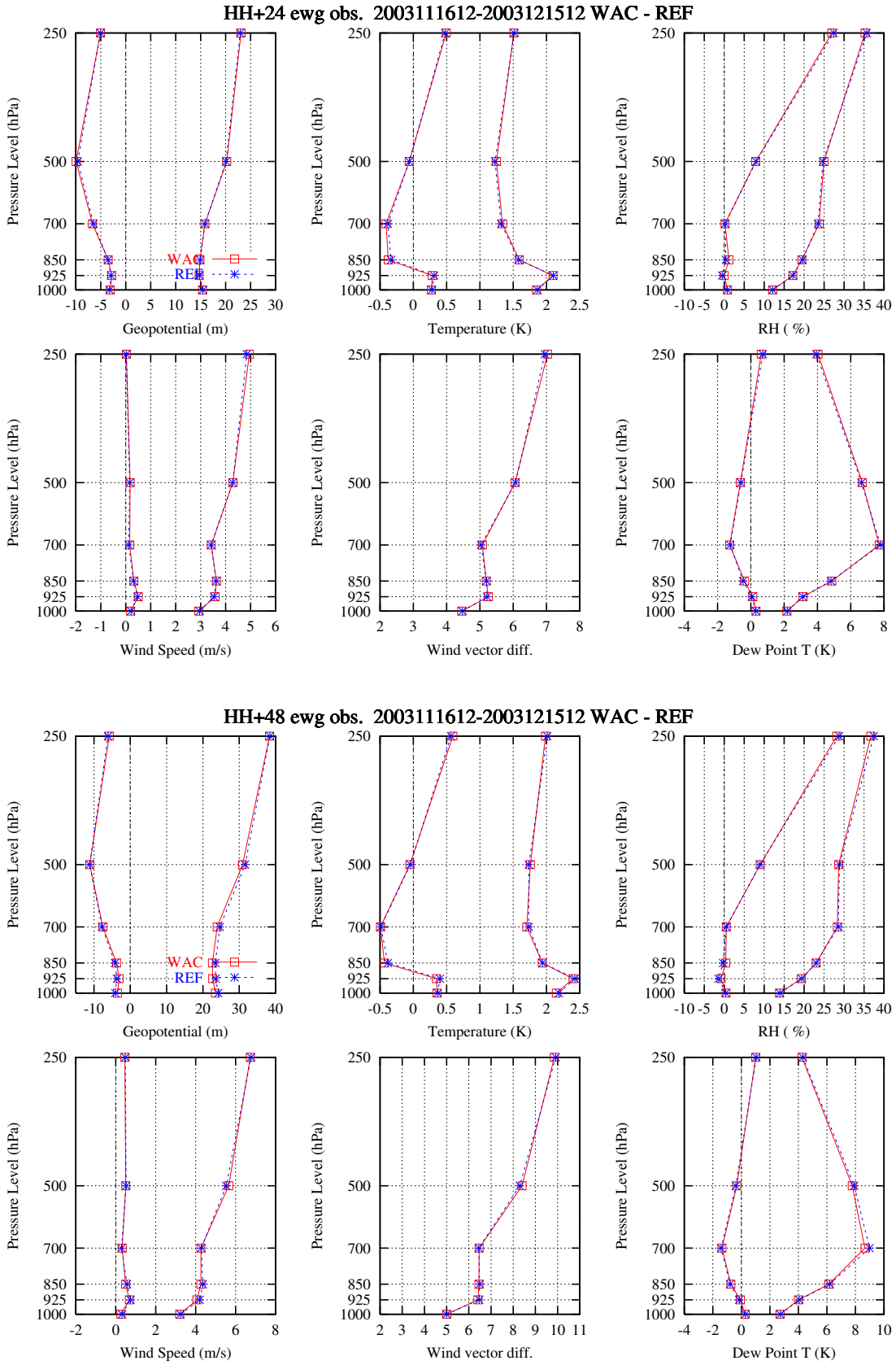


Figure 4: Vertical profiles of the verification scores at 24-hour forecast (*top*) and at 48-hour one (*bottom*) of the WAC and REF experiments.

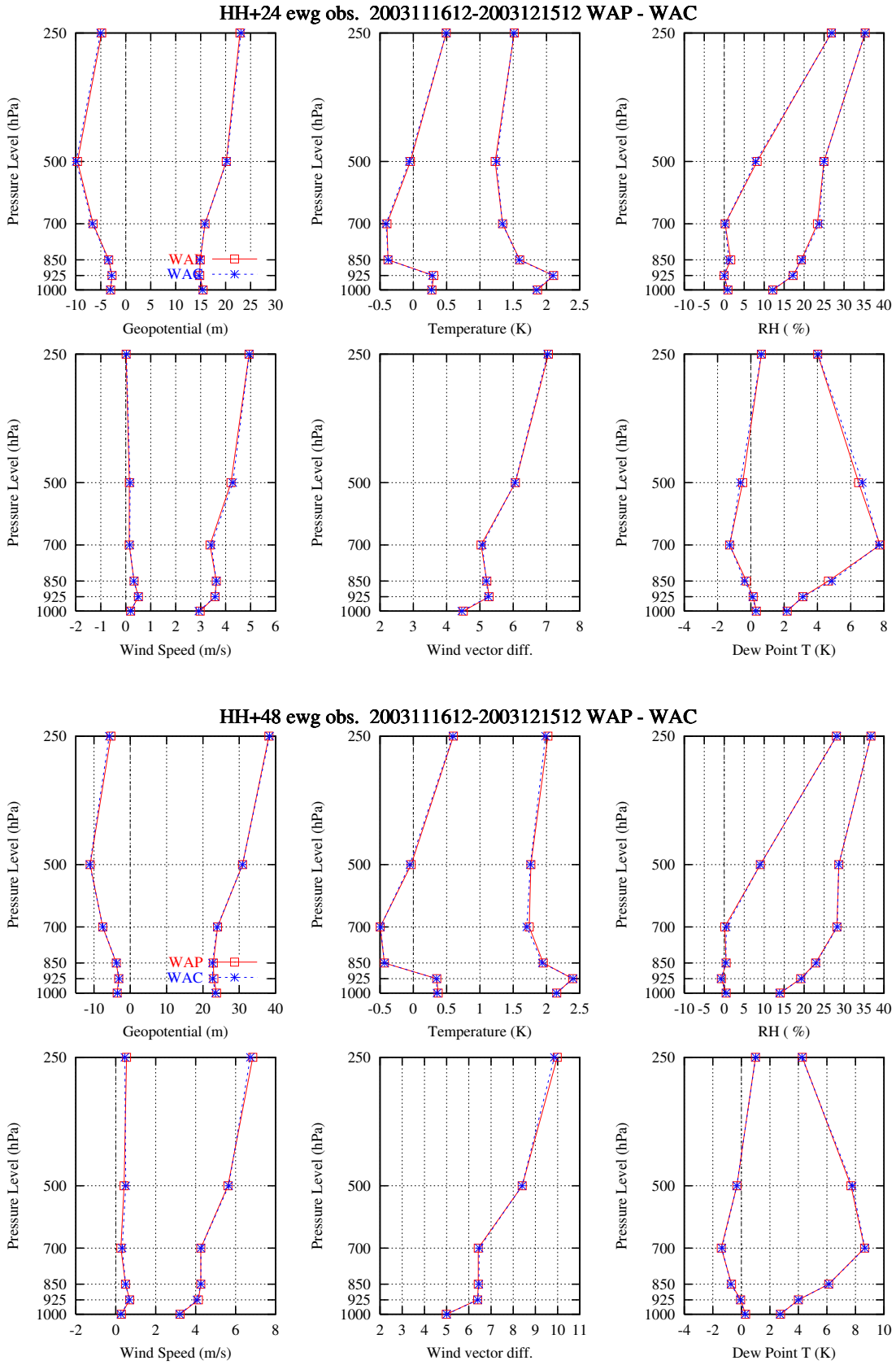


Figure 5: Vertical profiles of the verification scores at 24-hour forecast (*top*) and at 48-hour one (*bottom*) of the WAP and WAC experiments.